



UNIVERSITY OF LEEDS

This is a repository copy of *Microstructure Characterisation of Ni-75 at.% Al Raney Type Alloy as a Result of Cooling Rate and Chromium Doping*.

White Rose Research Online URL for this paper:

<http://eprints.whiterose.ac.uk/142348/>

Version: Accepted Version

Proceedings Paper:

Hussain, N, Mullis, AM orcid.org/0000-0002-5215-9959 and Forrester, J (2019) Microstructure Characterisation of Ni-75 at.% Al Raney Type Alloy as a Result of Cooling Rate and Chromium Doping. In: Proceedings. MRS 2018 Fall Meeting, 25-30 Nov 2018, Boston, MA. Materials Research Society .

Reuse

Items deposited in White Rose Research Online are protected by copyright, with all rights reserved unless indicated otherwise. They may be downloaded and/or printed for private study, or other acts as permitted by national copyright laws. The publisher or other rights holders may allow further reproduction and re-use of the full text version. This is indicated by the licence information on the White Rose Research Online record for the item.

Takedown

If you consider content in White Rose Research Online to be in breach of UK law, please notify us by emailing eprints@whiterose.ac.uk including the URL of the record and the reason for the withdrawal request.

Microstructure Characterisation of Ni-75 at.% Al Raney Type Alloy as a Result of Cooling Rate and Chromium Doping

Naveed Hussain, Andrew M Mullis, and Jennifer S Forrester

School of Chemical & Process Engineering, University of Leeds, Leeds LS2 9JT, UK.

ABSTRACT

The effect of cooling rate on the phase composition of gas atomized Raney type catalysts was studied using the Ni-75 at.% Al composition. The resulting particles were sieved into 3 standard size fractions and analysed using XRD with Rietveld refinement: as expected the three phases, Al_3Ni_2 , Al_3Ni , and $Al-Al_3Ni$ eutectic were identified. Differing phase compositions in the 3 size ranges were identified offering a possible explanation for varying catalytic activity with cooling rate, the higher cooling rates experienced by the smaller droplets allow less time for the peritectic conversion of Al_3Ni_2 to Al_3Ni to proceed. This in turn results in a more Al-rich residual liquid, increasing the volume fraction of eutectic. This was further confirmed when analysing the microstructure using SEM backscatter imaging. Al_3Ni_2 was found to be encased in a shell of Al_3Ni characteristic of peritectic reactions. The remainder of the alloy was found to consist of $Al-Al_3Ni$ eutectic. The SEM backscatter imaging also indicated that the larger particles displayed and a more globular structure than smaller particles. Similar Raney type Ni-75 at.% Al doped with 1.5 at.% Cr were synthesised using the same method and sieved into the same 3 standard size fractions. It was found that the Cr doped alloys exhibited a more dendritic character than the undoped samples in the corresponding size fraction, although the material still displayed an increasingly dendritic character with increasing cooling rate. The phase composition found by Rietveld refinement also followed a similar trend to the undoped samples with decreasing amounts of Al_3Ni formed at the higher cooling rates. However, significant amounts of an additional phase, $Al_{13}Cr_2$, were also observed. Rietveld refinement found that a larger amount of $Al_{13}Cr_2$ was present than could be accounted for by the addition of 1.5 at.% Cr. This can be explained by the substitution of Ni onto the Cr lattice, as confirmed by Rietveld refinement. $Al_{13}Cr_2$ was found to be located mostly at the boundary of the Al_3Ni and $Al-Al_3Ni$ eutectic phases during elemental mapping and quantitative image analysis of backscattered electron micrographs. This indicates that precipitation of $Al_{13}Cr_2$ is towards the end of the solidification process. The relatively large amounts of the Al-rich $Al_{13}Cr_2$ may explain the enhanced catalytic activity observed following leaching of Cr-doped Raney catalysts.

INTRODUCTION

Traditionally, a favoured choice for hydrogenation reactions, Raney Ni catalyst consists of approximately 68.5 at. % Al, which would result in a 50-50 wt% ratio of Al

and Ni. Coarse powders of Raney Ni are created by casting the alloy into ingots and then crushing.

The as-solidified precursor Al-Ni alloy is found to contain three distinct phases; Al_3Ni_2 (Space group: $P\bar{3}m1$ [1]), Al_3Ni (Space Group: $Pnma$ [1]) and an Al-Al₃Ni eutectic [2]. During cooling of the 68.5 at. % Al alloy the first phase to appear, at 1623 K, is AlNi. The remaining liquid will then react with the AlNi via the peritectic reaction at 1406 K to give Al_3Ni_2 . Irrespective of cooling rate, the AlNi phase is rarely found in the final microstructure [2]. In a study by Lengsdorf *et al*, *in-situ* time-resolved XRD was used to detect the first phase to form and it was concluded that Al_3Ni_2 is formed via the peritectic reaction [3], which must go to completion. The second peritectic reaction occurs at 1127 K, wherein the Al_3Ni_2 reacts with the remaining liquid to form Al_3Ni . This reaction is slower than the first peritectic reaction, with residual Al_3Ni_2 normally observed within the final microstructure. The last stage of solidification involves the residual liquid solidifying to an Al-Al₃Ni eutectic [4], occurring at 913 K.

For the hydrogenation of acetone, butyronitrile and sodium p-nitrophenolate the optimum level of Chromium in the Raney Ni alloy has been found to be 1.5 wt% [4]. An increase in catalytic activity was also found in a study by Bonnier *et al* where Al-Ni and Cr-Al alloys were mechanically mixed for the hydrogenation of acetophenone [5]. Chromium was also found to be strongly segregated to the surface in an oxidised state. Chromium oxide has been found to promote reactions such as the hydrogenation of carbonyl groups [4], inhibited by metallic aluminium [6]. For the hydrogenation of isophorone to dihydroisophorone it has been found that Cr segregated to the surface promoted catalytic activity, but for the reaction of dihydroisophorone hydrogenation it has been found to deactivate the Ni-Al catalyst [7]. Previously it has been assumed that Cr randomly substitutes for Ni due to their chemical similarity [5].

The IMPRESS project has investigated the effect of both rapid solidification and dopants on the catalytic activity of Raney Ni catalysts. Particle sizes of 38-212 μm were rapidly solidified via high pressure gas atomisation, with estimated cooling rates between 200 – 10000 K s⁻¹ [8] and the catalytic activity was compared with a benchmark for the hydrogenation of nitrobenzene (3.5 mol kg⁻¹ min⁻¹). In the 106-150 μm size fraction, gas atomised powders of the 50-50 wt% composition showed an activity of only 1.4 mol kg⁻¹ min⁻¹, whereas for a 75 at. % Al catalyst the activity was 4.8 mol kg⁻¹ min⁻¹. Moreover, the catalytic activity for the hydrogenation of nitrobenzene was found to increase from 4.8 mol kg⁻¹ min⁻¹ to 11.6 mol kg⁻¹ min⁻¹ with the addition of 1.5 at.% Cr to a 75 at. % Al alloy in the 106-150 μm size fraction. In the standard 50-50 wt. % cast-crush alloy the change in activity was from 3.5 mol kg⁻¹ min⁻¹ to 7.35 mol kg⁻¹ min⁻¹ [9]. It was not established why the addition of Cr improved the catalytic activity.

EXPERIMENTAL PROCEDURE

Close coupled gas atomisation was used to produce two batches of particulate material with the following composition 25% Ni + 75% Al and 23.5% Ni + 75% Al + 1.5% Cr (all at.-%). Full details of the experimental procedure are given in [8]. The solidified particulate samples were then subject to sieving into the following size fractions: 53 μm < 75 μm , 75 μm < 106 μm and 150 μm < 212 μm . The estimated cooling rates are 1800, 1000 and 320 K s⁻¹ respectively [8].

Samples of each size fraction were mounted into a low-background silicon sample holder as a flat layer of powder to undergo XRD using a Bruker D8 diffractometer with Cu-K_α radiation. The resulting XRD patterns were compared to the International Centre for Diffraction Data (ICDD) database using the HighScore program in order to

identify the phases present. The General Structure Analysis Software (GSAS) program [10] with the EXPGUI [11] interface was used to carry out Rietveld refinement.

The particulate samples were also mounted in TransOptic™ resin before being ground and polished using 6 µm, 3 µm and 1 µm diamond paste. A layer of carbon was used to sputter coat the samples to minimise charging during Scanning Electron Microscopy (SEM). The Hitachi SU8230 microscope was used in backscattered detection mode to analyse the microstructure, and Electron Dispersive X-Ray Spectroscopy (EDX) was used to map Cr within the microstructure.

RESULTS

CALPHAD Modelling

The CALPHAD modelling software package MTDATA [12] with version 4.3 of the SGTE database was used to calculate a Scheil solidification sequence for $\text{Al}_{75}\text{Ni}_{(25-x)}\text{Cr}_x$. Three additional compounds were identified as potentially present: Al_4Cr , predicted to form via primary solidification direct from the melt (1139 K); $\text{Al}_{11}\text{Cr}_2$, predicted to form via a peritectic reaction between the Al_4Cr phase and the remaining liquid at 1069 K and $\text{Al}_{13}\text{Cr}_2$, predicted to form via the final peritectic reaction between $\text{Al}_{11}\text{Cr}_2$ and the residual melt at 983 K.

XRD Measurements.

XRD analysis found that the three predicted phases, Al_3Ni_2 , Al_3Ni and Al (in the Al-Al₃Ni eutectic), exist in all particle size fractions, including all Cr doped samples. The additional peaks observed in all size fractions of Cr-doped AlNi were identified as a single monoclinic $\text{Al}_{13}\text{Cr}_2$ phase (space group: $C2/m$ [13]) and consistent, stable phase fraction data was obtained. No evidence of either Al_4Cr or $\text{Al}_{11}\text{Cr}_2$ was found, which would suggest if the solidification sequence followed the Scheil calculation, then both of the Al-Cr peritectic reactions were able to go to completion.

Weight fractions acquired from the Rietveld refinements are presented in Table I. The smaller particles appear to contain more Al_3Ni_2 and less Al_3Ni . The amount of Al eutectic also increases with smaller particles which agrees with the expectation that the Al_3Ni_2 to Al_3Ni peritectic has less time to proceed at higher cooling rates.

The abundance of $\text{Al}_{13}\text{Cr}_2$ in the Cr doped particles can also be seen in Table I. It is clear there is significant amounts of this phase, exceeding the maximum weight fraction possible (approx. 9.5 wt.%) without substitution of Ni for Cr in the $\text{Al}_{13}\text{Cr}_2$ lattice. When Rietveld refinement was conducted with the assumption that Ni substitutes into the Cr lattice all the Cr deficiencies within the $\text{Al}_{13}\text{Cr}_2$ were accounted for by Ni.

Table 1. Weight fractions of each phase in Al-25 at.% Ni and Al-23.5 at.% Ni-1.5 at.% Cr obtained using Rietveld refinement of XRD data.

Size fraction	Weight %				
	Al ₃ Ni ₂	Al ₃ Ni	Al eutectic	Al ₁₃ Cr ₂	
Al-25 at.% Ni	150µm < 212µm	33.5	53.8	12.7	N/A
	75µm < 106µm	34.1	50.4	15.5	N/A
	53µm < 75µm	36.3	47.3	16.4	N/A
Al-23.5 at.% Ni -1.5 at. %Cr	150µm < 212µm	29.1	45.2	9	16.8
	75µm < 106µm	30.4	38.9	13.7	16.9
	53µm < 75µm	32.9	37.1	13.4	16.6

SEM Microstructure characterisation

The SEM micrographs of the undoped and Cr doped Raney powder can be seen in Figures 1 a and b, where three distinct phases are visible in backscatter mode, appearing light grey (Al₃Ni₂, most Ni-rich phase), dark grey (Al₃Ni) and black (eutectic, least Ni-rich phase). Typical with peritectic reactions there is a characteristic core shell morphology as Al₃Ni surrounds the Al₃Ni₂ phase. The undoped samples also display a similar morphology of dendrites but the dendritic character of the Cr doped samples appears overall more developed than the undoped samples.

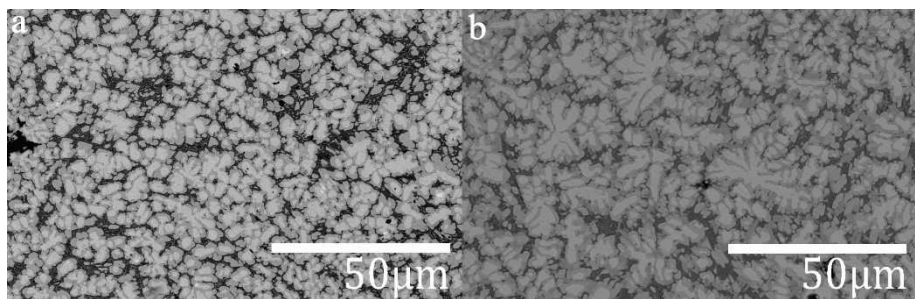


Figure 1. SEM backscatter images of a) Al-25 at.% Ni and b) Al-23.5 at.% Ni-1.5 at. % Cr alloys at 150µm<212µm particle size fraction.

Cr localisation can be seen in figure 2a as an EDX map for Cr is overlaid onto a backscattered micrograph of a Cr doped particle. The Cr is co-located with the Al₃Ni phase and mostly present on the boundary between Al₃Ni and the Al eutectic. The location of Cr suggests that the Al₁₃Cr₂ is formed directly from the melt, probably towards the end of Al₃Ni growth, and not from a series of peritectic reactions as predicted by the Scheil calculation, which would co-locate the Cr-rich phase with the high temperature Al₃Ni₂ phase. The location Al₁₃Cr₂ as identified by backscatter grey level can be seen in figure 2b and corresponds to the localisation of Cr illustrated in figure 2a. The pixel count of the corresponding grey-levels is also in agreement to the phase fraction as this represents a 21 vol.% of the 212-150 µm sieve fraction. For comparison, converting the data in Table I to

volume %, 16.8 wt.% $\text{Al}_{13}\text{Cr}_2$ is 20.1 vol.%. This level of agreement was also found with the other 2 size fractions of Cr doped samples.

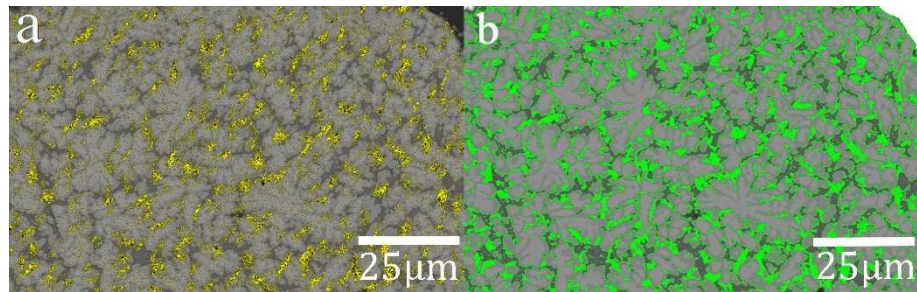


Figure 2. SEM backscatter images for $150\mu\text{m} < 212\mu\text{m}$ size fraction of the Al-23.5 at.% Ni-1.5 at.% Cr alloy a) overlaid with Cr EDX maps illustrating Cr localisation within the microstructure, and b) displaying grey levels 83-101 highlighted in green.

Four point EDX measurements were taken from the $\text{Al}_{13}\text{Cr}_2$ phase of all three size fractions of Cr doped samples. The results are presented in Table II. Based on a mass balance calculation, the amounts of Cr found within the $\text{Al}_{13}\text{Cr}_2$ phase agrees with the amount of Cr available, given the volume fraction of $\text{Al}_{13}\text{Cr}_2$ present. However, the amount of Al found within the phase does not agree with the notional stoichiometry of the phase, wherein 86.6 at. % would be expected. We conjecture that Ni may also substitute for Al as well as Cr, although this could also be an artefact because of the relatively large interaction volume in the EDX process which may include Ni from nearby phases.

Table 2. The elemental composition of $\text{Al}_{13}\text{Cr}_2$ for each sample size fraction of Al-23.5 at.% Ni-1.5 at.% Cr obtained using Point EDX analysis.

Spectrum	Atomic % (Standard error)		
	$150\mu\text{m} < 212\mu\text{m}$	$75\mu\text{m} < 106\mu\text{m}$	$53\mu\text{m} < 75\mu\text{m}$
Al	76.92 (3.19)	74.28 (9.17)	82.8 (7.43)
Cr	8.31 (5.83)	6.55 (2.92)	6.65 (2.39)
Ni	14.78 (5.83)	19.18 (10.65)	10.56 (5.33)

DISCUSSION

The cooling rate, as a result of particle size, has an effect on the final microstructure; as the particle size increases the fraction of Al_3Ni_2 present decreases while that of Al_3Ni increases. This may possibly be due to the slower cooling rate in the larger particles allowing more time for the $\text{Al}_3\text{Ni}_2 \rightarrow \text{Al}_3\text{Ni}$ peritectic to take place.

The more dendritic character of the Cr doped samples, compared to the undoped samples, may be attributed to an additional solute flux, as no Cr is found to be co-located in the primary Al_3Ni_2 phase.

The additional phase, $\text{Al}_{13}\text{Cr}_2$, in the Cr doped samples is found to contain all the Cr within the alloy, which conclusively refutes the assertion that Cr randomly substitutes for Ni [5]. The spatial location of the $\text{Al}_{13}\text{Cr}_2$ phase itself suggests that it is not formed via

the series of peritectics predicted in the Scheil solidification sequence but instead directly from the melt with all the Cr is retained within the liquid during the initial growth of Al₃Ni₂.

Leaching of the Cr doped powders within this study would give Cr on the surface of the activated catalyst as Al₁₃Cr₂ is the first phase to be encountered after the Al-eutectic is removed, this would not only give a surface Cr coating, as observed by Bonnier *et al.* [5], but since Al₁₃Cr₂ is more Al-rich than Al₃Ni it is also expected to give a more open nano-porous structure. This would allow further development into Raney type alloys as catalytic activity is likely to be enhanced by any phase that is Al-rich (> 85 at. %).

References:

- [1] M. Ellner, U. Kattner and B. Predel, Journal of the Less Common Metals. 87 (2), 305, (1982).
- [2] F. Devred, A. H. Gieske, N. Adkins, U. Dahlborg, C. M. Bao, M. Calvo-Dahlborg, J. W. Bakker and B. E. Nieuwenhuys, Applied Catalysis A: General. 356, 154-161, (2009).
- [3] R. Lengsdorf, D. Holland-Moritz and D. M. Herlach, Acta Materialia. 62, 365-367, (2009).
- [4] F. Devred, IMPRESS project, (2004).
- [5] J. M. Bonnier, J. P. Damon and J. Masson, Applied Catalysis. 42 (2), 285-297, (1988).
- [6] T. Koscielski, J. M. Bonnier, J. P. Damon and J. Masson, Applied Catalysis. 49 (1), 91-99, (1989).
- [7] M. Pisarek, M. Łukaszewski, P. Winiarek, P. Kedzierzawski and M. Janik-Czachor, Catalysis Communications. 10, 213-216, (2008).
- [8] A. M. Mullis, L. Farrell, R. F. Cochrane and N. J. Adkins, Metallurgical and Materials Transactions B. 44B (4), 992-998, (2013).
- [9] IMPRESS, Intermetallic Processing in Relation to Earth and Space Solidification, EU Framework VI (Integrated) Project # NMP3-CT-2004-500635-2.
- [10] A. C. Larson and R. B. Von Dreele, General Structure Analysis System (GSAS), Los Alamos National Laboratory, (2004).
- [11] B. H. Toby, Journal of Applied Crystallography. 34, 210-213, (2001).
- [12] R. H. Davies, A. T. Dinsdale, J. A. Gisby, J. A. J. Robinson and S. M. Martin, CALPHAD. 26 (2), 229-271, (2002).
- [13] M. J. Cooper, Acta Crystallographica. 13 (3), 257, (1960).